Bringing the ocean into the laboratory to probe the chemical complexity of sea spray aerosol

Kimberly A. Prather[a,b,1], Timothy H. Bertram[a], Vicki H. Grassian[c], Grant B. Deane[b], M. Dale Stokes[b], Paul J. DeMott[d], Lihini I. Aluwihare[b], Brian P. Palenik[b], Farooq Azam[b], John H. Seinfeld[e], Ryan C. Moffet[f], Mario J. Molina[a,b], Christopher D. Cappa[g], Franz M. Geiger[h], Gregory C. Roberts[b,i], Lynn M. Russell[b], Andrew P. Ault[c], Jonas Baltrusaitis[c,2], Douglas B. Collins[a], Craig E. Corrigan[b], Luis A. Cuadra-Rodriguez[a], Carlena J. Ebben[h], Sara D. Forestieri[g], Timothy L. Guasco[a], Scott P. Hersey[e], Michelle J. Kim[b], William F. Lambert[b], Robin L. Modini[b], Wilton Mui[e], Byron E. Pedler[b], Matthew J. Ruppel[a], Olivia S. Ryder[a], Nathan G. Schoepp[a], Ryan C. Sullivan[d,3], and Defeng Zhao[a,4]

[a]Department of Chemistry and Biochemistry and [b]Scripps Institution of Oceanography, University of California at San Diego, La Jolla, CA 92093; [c]Department of Chemistry, University of Iowa, Iowa City, IA 52242; [d]Department of Atmospheric Science, Colorado State University, Fort Collins, CO 80523; [e]Division of Chemistry and Chemical Engineering, California Institute of Technology, Pasadena, CA 91125; [f]Department of Chemistry, University of the Pacific, Stockton, CA 95211; [g]Department of Civil and Environmental Engineering, University of California, Davis, CA 95616; [h]Department of Chemistry, Northwestern University, Evanston, IL 60208; and [i]Centre National de Recherches Météorologiques, 31057 Toulouse, France

Edited* by Mark H. Thiemens, University of California at San Diego, La Jolla, CA, and approved March 21, 2013 (received for review January 10, 2013)

The production, size, and chemical composition of sea spray aerosol (SSA) particles strongly depend on seawater chemistry, which is controlled by physical, chemical, and biological processes. Despite decades of studies in marine environments, a direct relationship has yet to be established between ocean biology and the physicochemical properties of SSA. The ability to establish such relationships is hindered by the fact that SSA measurements are typically dominated by overwhelming background aerosol concentrations even in remote marine environments. Herein, we describe a newly developed approach for reproducing the chemical complexity of SSA in a laboratory setting, comprising a unique ocean-atmosphere facility equipped with actual breaking waves. A mesocosm experiment was performed in natural seawater, using controlled phytoplankton and heterotrophic bacteria concentrations, which showed SSA size and chemical mixing state are acutely sensitive to the aerosol production mechanism, as well as to the type of biological species present. The largest reduction in the hygroscopicity of SSA occurred as heterotrophic bacteria concentrations increased, whereas phytoplankton and chlorophyll-*a* concentrations decreased, directly corresponding to a change in mixing state in the smallest (60–180 nm) size range. Using this newly developed approach to generate realistic SSA, systematic studies can now be performed to advance our fundamental understanding of the impact of ocean biology on SSA chemical mixing state, heterogeneous reactivity, and the resulting climate-relevant properties.

clouds | marine aerosols | biologically active | cloud condensation nuclei | ice nucleation

Atmospheric aerosols have a profound impact on climate by directly interacting with incoming solar radiation, as well as by serving as the seeds that nucleate clouds (1). Natural aerosol sources, which include the oceans, deserts, and wildfires, contribute 90% (mass/mass) to atmospheric aerosols, with sea spray and dust representing the two largest contributors. Given the vast coverage of the Earth's surface by the oceans, the impact of sea spray aerosol (SSA) on the Earth's radiation budget is a critical area of ongoing climate investigations. The current uncertainties associated with the total radiative forcing by anthropogenic aerosols are much larger than those for greenhouse gases (2). To reduce these uncertainties, the impact of large natural sources, such as sea spray, must be better understood, because the difference between the total forcing and the forcing from natural sources will provide a critical constraint on the forcing from anthropogenic aerosols (3). Primary SSA, formed at the air/sea interface through bubble-mediated processes (4), dominates the natural aerosol burden in most marine environments. However, it has become increasingly difficult to unravel contributions from anthropogenic and marine sources even in remote marine environments (3, 5). Global models that parameterize nascent SSA disagree by more than two orders of magnitude in the absolute number flux (global, annual average) (6–8) and require major assumptions regarding nascent SSA size and single particle mixing state (6). Currently, accurate representation of SSA in climate models is limited by an incomplete understanding of the dependence of SSA properties on physical, biological, and chemical processes occurring in the ocean (8).

Previous field and laboratory studies have shown that SSA is a complex mixture of sea salt (SS) and an array of organic species with differing solubilities (4, 9, 10). Most SSA field and laboratory measurements focus on absolute mass concentrations and the enrichment of organic compounds relative to salts (e.g., ref. 11), with the assumption that salts and organic species are equally distributed among all particles of a given size (internally mixed). The chemical associations between species within individual SSA particles (or chemical mixing state) is directly influenced by ocean physics, biology, and chemistry, and ultimately control both particle hygroscopicity (12) and the number of particles that can act as cloud condensation nuclei (CCN) and ice nuclei (IN) (13). The few studies that focus on single particle measurements suggest that SSA cannot be completely described as internally mixed (9, 14, 15) but, rather, as a distribution of chemically distinct particle types (externally mixed). The current view of SSA particle mixing state in the size range most important for cloud formation (<200 nm) is controversial (16). Although some studies suggest a large fraction of salt particles below 200 nm, others report salts are nearly absent and SSA becomes increasingly enriched with organic species at these small sizes (e.g., ref. 11). Some suggest individual SSA

Author contributions: K.A.P., T.H.B., V.H.G., and M.J.M. designed research; G.B.D., M.D.S., P.J.D., A.P.A., D.B.C., C.E.C., L.A.C.-R., C.J.E., S.D.F., T.L.G., M.J.K., R.L.M., W.M., M.J.R., O.S.R., R.C.S., and D.Z. performed research; G.B.D., M.D.S., L.I.A., B.P.P., F.A., J.H.S., G.C.R., L.M.R., W.F.L., B.E.P., and N.G.S. contributed new reagents/analytic tools; K.A.P., G.B.D., M.D.S., P.J.D., J.H.S., R.C.M., C.D.C., F.M.G., A.P.A., J.B., D.B.C., C.E.C., L.A.C.-R., C.J.E., T.L.G., S.P.H., W.M., M.J.R., R.C.S., and D.Z. analyzed data; and K.A.P., T.H.B., V.H.G., and C.D.C. wrote the paper.

The authors declare no conflict of interest.

*This Direct Submission article had a prearranged editor.

[1]To whom correspondence should be addressed. E-mail: kprather@ucsd.edu.

[2]Present adress: PhotoCatalytic Synthesis Group, Faculty of Science and Engineering, University of Twente, 7522 NB, Enschede, The Netherlands.

[3]Present address: Center for Atmospheric Particle Studies, Carnegie Mellon University, Pittsburgh, PA 15213.

[4]Present address: Institute of Energy and Climate: Troposphere (IEK-8), Forschungszentrum Juelich, D-52428 Juelich, Germany.

This article contains supporting information online at www.pnas.org/lookup/suppl/doi:10.1073/pnas.1300262110/-/DCSupplemental.

particles may be even more complex and composed of organized structures formed by the complexation of inorganic salts with organic species produced by biological processes (17, 18). Even though climate impacts of SSA are expected to depend on particle composition as a function of size, no study to date has probed how SSA mixing state changes as a function of seawater conditions, a major focus of this investigation.

The goal of this study is to develop a unique approach that will allow us to bridge results from laboratory and field studies of SSA by accurately reproducing the chemical complexity and associations (i.e., mixing state) of real-world SSA for controlled studies of reactivity, water uptake, and climate-relevant properties. Here, we describe a newly developed approach that brings the chemical complexity of the ocean-atmosphere system into the laboratory (Fig. S1). Simultaneous measurements of seawater, SSA size distributions, and size-resolved single particle chemical composition are made in an enclosed ocean-atmosphere wave channel equipped with breaking waves and natural seawater. This facility permits studies of the impact of seawater composition on SSA properties under controlled and well-characterized biological conditions (19). This paper is divided into three sections, each detailing the progression of advances: (*i*) measurements of nascent SSA produced by breaking waves in a laboratory setting, demonstrating the extreme sensitivity of the SSA size distribution to the bubble size distribution, and hence the SSA production mechanism; (*ii*) size-resolved associations between inorganic and organic species within individual SSA particles (i.e., chemical mixing state), covering two orders of magnitude in size from 30 nm to 3 μm, by integrating the results from several single particle techniques, including aerosol TOF mass spectrometry (ATOFMS), scanning tunneling X-ray microscopy (STXM), and transmission electron microscopy (TEM); and (*iii*) a mesocosm seawater experiment to explore the dependence of SSA chemical mixing state and physicochemical properties on ocean biology over a range of conditions representative of the open ocean, by adding well-characterized phytoplankton and bacteria mixtures and allowing the chemistry to evolve over a 5-d period (20–22).

Generation and Reproduction of SSA Size Distributions

In the SSA particle production process, several key interfaces ultimately determine the surface species and morphology of SSA. As a bubble rises through the water column, different hydrophobic molecules are attracted to the air/bubble interface, offering the first level of chemical selectivity (4, 23). Because a bubble bursts at the ocean surface, the sea surface microlayer represents a second critical interface where chemical partitioning occurs (24). Finally, as individual droplets undergo drying under lower relative humidity (RH) conditions, the resulting SSA particle morphology will depend on surface interactions. Biological processes play a significant role in forming the species that each bubble encounters in the water column as well as those residing in the sea surface microlayer (4, 23). Thus, each step of the SSA production process must be properly replicated or erroneous conclusions will be drawn in any subsequent heterogeneous reactivity and water uptake studies on SSA.

SSA is created when bubbles entrained by breaking waves burst at the ocean surface (4). Two distinct mechanisms control aerosol production: the rapid retraction and disintegration of the thin fluid film that caps the bubble (film drops) and the breakup of a reactionary jet (jet drops), with their relative contributions depending on the size spectrum of the bubbles (8). Accurate representation of these mechanisms in the laboratory is a critical requirement for reproducing the size distribution and chemical composition of nascent SSA. However, the majority of previous laboratory studies generated SSA using sintered glass filters and typically did not measure bubble size distributions (25). In the experiments described herein, SSA was generated using three different interchangeable systems: (*i*) sintered glass filters (25), (*ii*) a pulsed-plunging waterfall, and (*iii*) continuous wave breaking at 0.6 Hz, all operating within a sealed 33-m wave channel filled with natural seawater pumped directly from the Pacific Ocean (*SI Text*, section 1).

In situ acoustic and optical measurements of bubble size distributions (dN/dr_B, where r_B = bubble radius; Fig. 1*A*) show consistency between generation mechanisms up to approximately $r_B = 0.7$ mm but deviate above 1 mm. Aerosol production is sensitive to total foam area and the distribution of cell sizes within the foam (26). Multiplying the bubble size distribution by the potential to generate surface film (roughly $2\pi r_B^2$) yields a peak in the distribution at the Hinze scale, as observed in previous open ocean studies ($a_H = 1.3$ mm; a is the bubble radius and H stands for Hinze, Fig. 1*A*) (19). Because most foam from breaking waves comes from bubbles around this scale, the level and slope of the bubble distribution at this scale must be reproduced by any generation mechanism used as a surrogate for natural wave breaking. It has been reported that the vast majority of submicrometer SSA particles that can act as CCN emanate from film drops that are produced by larger bubbles with sizes above 1 mm (27–29). Importantly, the measured bubble spectrum for the breaking waves used in this study matches the shape and Hinze scale of bubble spectra measured previously for open ocean breaking waves (19). Previous studies using plunging jets have produced similar bubble size distributions only up to radii of 0.57 mm (30). Thus, herein breaking waves with bubble size distributions representative of open ocean conditions are used to produce nascent SSA with atmospherically representative size distributions and chemical mixing states, as described below.

Nascent SSA size distribution ($dN/d\log d_p$, where d_p is particle physical diameter) from the three production mechanisms were measured at 15 ± 10% RH (Fig. 1*B*). The mode of the probability density function of the particle number distribution is 162 ± 21 nm (1σ) for SSA generated using breaking waves. The number distribution is broad, extending from 10 nm to 5 μm. The plunging waterfall produces SSA with a similar size distribution to that produced by breaking waves, which is expected, given the similar bubble spectra produced by the two generation methods. In contrast, SSA produced using two sizes of sintered glass filters or frits commonly used in previous experiments (25) exhibits a much narrower size distribution, reflecting the different bubble size spectrum produced by this method (compare with Fig. 1*A*).

The measured size distribution peaks at the lower end of the accumulation mode (~162 nm) as observed in previous studies in marine environments (6, 8). This distribution shows only a small contribution from particles in the smaller Aitken mode in the sub–100-nm size range. This distribution is in contrast to previous marine field studies, including those that used frits to produce SSA, which show another mode below 100 nm (8, 25, 31–33). As described, it is extremely difficult to separate out contributions

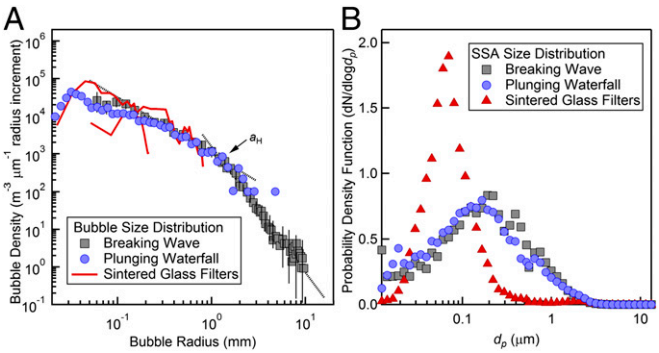

Fig. 1. (*A*) Bubble radius distributions for breaking waves (gray squares), plunging waterfall (blue circles), and sintered glass filters (red line). [Reproduced with permission from ref. 19 (Copyright 2002, Macmillan Publishers)]. (*B*) Probability density function of the resulting SSA number distributions ($dN/d\log d_p$, with the d_p at 15 ± 10% RH) produced by these three methods. The SSA distribution recovered from the plunging waterfall is consistent with that produced by breaking waves, whereas the SSA distribution by the sintered glass filters (red triangles) is considerably narrower.

from background aerosols and other secondary particle formation processes that have been shown to occur in marine environments (3, 5, 34). The ability to produce and measure an extremely stable nascent SSA size distribution over a broad range of biological conditions demonstrates the advantage of performing these experiments in a laboratory setting, where contributions from other sources and secondary processes can be eliminated. Thus, future studies will probe the effects of seawater temperature, wind, and biological conditions to determine if the Aitken mode can be produced under different conditions (i.e., phytoplankton bloom) or whether it is entirely attributable to background and secondary processes.

The motivation for the development of this unique ocean-atmosphere facility is to be able to perform systematic control studies that help provide a better understanding of the large observed variability in SSA size and composition distributions measured over the ocean, as well as associated variations in cloud properties (6). Thus, it is critical to use a production process that replicates the full bubble size distributions, including larger sizes, to generate SSA with a realistic distribution of particle sizes and compositions.

SSA Chemical Mixing State

Our first experiments used natural seawater drawn directly from Pacific coastal waters into the wave channel. Over the course of 10 d, after adding multiple varieties of phytoplankton cultures and filling the tank on different days with natural seawater, very little change was observed in the overall SSA composition or hygroscopicity. To explore the influence of ocean biological and chemical complexity on emitted SSA properties, a 5-d mesocosm experiment was then conducted wherein natural seawater was doped sequentially with well-characterized ZoBell growth medium, bacteria (*Alteromonas spp.* and *Pseudoalteromonas atlantica*), and phytoplankton (*Dunaliella tertiolecta*) cultures (Table S1). The time series for heterotrophic bacteria, phytoplankton, chlorophyll-*a*, and total organic carbon (TOC) concentrations are shown in Fig. 2. The primary objective of these experiments was not to simulate large-scale oceanic phytoplankton blooms that occur in limited regions of the ocean (11) but, instead, to detail how variations in and interactions between biological species alter SSA properties under conditions generally representative of the mean ocean state [i.e., TOC = 60–70 μM (20), bacteria concentrations of 5×10^5–3×10^6 cells·mL^{-1} (21), chlorophyll-*a* concentrations of 0.15–1 mg·m^{-3} (22)]. SSA was produced using continuous wave breaking, where measurements of background particle levels within the wave channel indicate that contamination from background aerosol contributed ~10% on average (up to 20% for short isolated periods) to the measured particle number concentrations (Fig. S2). Both SSA number concentrations and size distributions were exceptionally stable [N_{total} = 145 ± 20 particles·cm^{-3} and d_p (mode) = 162 ± 21 nm (1σ)] across the entire 5-d mesocosm experiment (Figs. S2 and S3) and showed very little variation even as bacteria, phytoplankton, chlorophyll-*a*, and TOC concentrations changed (Fig. 2).

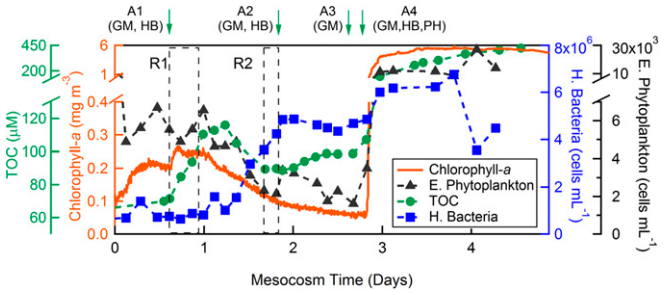

Fig. 2. Concentrations of seawater TOC (green circles), chlorophyll-*a* (orange line), heterotrophic bacteria (blue squares), and photosynthetic eukaryotic phytoplankton (black triangles) measured over the 5-d mesocosm experiment. Times for the four major additions of growth medium (GM), heterotrophic bacteria (HB), and phytoplankton (PH) are noted (A1–A4) with green arrows (*SI Text*, section 2.1 and Table S1). Dashed boxes mark two sampling regions (R1 and R2).

The mixing state of nascent SSA during the mesocosm experiment was examined using a combination of particle morphology and chemical heterogeneity measurements of individual particles, determining the size-resolved number fractions of chemically distinct particle types. Integration of microscopy and MS data of individual SSA particles reveals four predominant SSAs that persist throughout all experiments conducted (Fig. 3*A*), although the size-dependent relative number fractions vary over time (Fig. 4 *A* and *B*). The four individual particle types were defined based on both physical shape and chemical signatures (*SI Text*, section 4). They can be categorized as inorganic salts (types 1 and 2), biological (type 3), and organic (type 4) particles (Table S2), where the labels reflect the most dominant signals in the individual particles. A minor fraction of particles composed of unique signatures, each in negligible (<1%) abundance, and background aerosols were also detected. These particles were grouped together as a separate category referred to as Other (gray; Fig. 3*A* and *SI Text*, section 4.3.3). The relative fractions of the four major particle types show a strong size dependence [aerodynamic diameter (d_a) = 30–3,000 nm], with externally mixed particle populations spanning from inorganic salts dominating the largest sizes to mostly organic particles at the smallest sizes (Fig. 3*A*). It is important to note that all particle measurements discussed here describe nascent SSA, sampled less than 30 s following production, thus eliminating subsequent chemical and atmospheric processing of these particles, which are processes that have been shown to make major contributions in field observations to the composition of marine aerosols (35).

Supermicrometer particles are dominated by SS particles, with one type containing the typical inorganic salts dominated by NaCl (SS, type 1) and a second type (type 2) in which SS is mixed with organic carbon (SS-OC; Fig. S4). Individual SS-containing particles display spatial heterogeneity, with clear structural differences in the surface vs. inner regions of the particles. Larger type 1 particles show a cubic NaCl structure in microscopy analysis, and many type 2 (SS-OC) particles have an additional visible ring of Mg^{2+} on their surface, which becomes more common in smaller submicrometer particles (Fig. S5). One explanation for these rings is that they form when more soluble species, such as magnesium chloride, dehydrate last under vacuum in the electron microscope; however, this layered structure is also observed in the ATOFMS, which does not completely dry out the particles. We hypothesize that these rings serve as indicators of surface interactions between organic species and inorganic cations, as shown previously in laboratory studies of model inorganic/organic systems (36). A unique finding in this study is the presence of two distinct populations of nascent SS particles, supermicrometer particles dominated by NaCl showing cubic structures and smaller submicrometer salt particles relatively enriched in Mg^{2+} and organic species. This finding has significant ramifications for heterogeneous reactivity and water uptake studies. Additionally, a notable fraction of supermicrometer particles (type 3) had common biological markers, including organic-nitrogen species and phosphate in the negative ion mass spectra, coupled with Mg^{2+} and oftentimes transition metals in the positive ion mass spectra (37). Type 3 particles are likely biological particles, possibly bacteria, which have been shown to become enriched in the bubble bursting process (4, 23). These represented up to 17% of the supermicrometer particles, similar to the abundances previously reported for biological particles in marine environments (38).

Submicrometer SSA particles were composed of two externally mixed particle types, SS-OC (type 2) and organic dominated particles with no detectable chloride (type 4), as determined by TEM energy-dispersive X-ray analysis. Further details on the mixing state of organic and inorganic species within smaller type 4

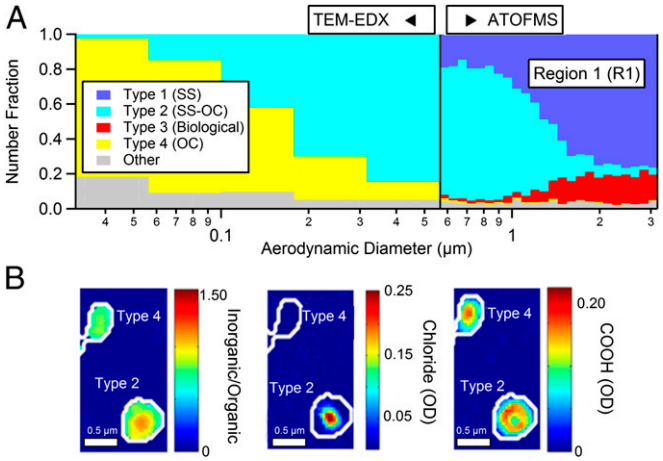

Fig. 3. (*A*) Size-resolved chemical mixing state for R1 (Fig. 2). Integration of two single particle analysis methods [TEM with energy-dispersive X-ray (EDX) analysis < 562 nm and ATOFMS > 562 nm] shows the existence of four major particle types. (*B*) STXM chemical spatial maps of the two most dominant submicrometer particle types (types 2 and 4) highlight the differences in the inorganic-to-organic ratios (*Left*), abundance of chloride (*Center*), and carboxylates (*Right*).

submicrometer individual particles were obtained with STXM (Fig. 3*B*). These particles were composed of homogeneously mixed organic species (e.g., carboxylate) combined with Na^+, Ca^{2+}, sulfur, and Mg^{2+} but distinctly lacking chloride. These type 4 particles represent the most abundant type below 180 nm, consistent with previous observations showing an increase in insoluble organic species at the smallest sizes (39), and are believed to be hydrophobic colloidal or gel particles (40). Particles composed primarily of insoluble organic compounds have been hypothesized to form when long-chain polymeric bioorganic species, such as carbohydrates, proteins, and lipids, bridge with divalent ions, including Ca^{2+} and Mg^{2+}, to form stable collapsed structures (40).

Chemical Biology Impacts on SSA Chemical Mixing State

During the first 2 d of the mesocosm experiment, an increase occurred in the relative fraction of type 4 OC-dominated particles in the 60–180 nm (d_a) range (Fig. 4*A*; 0.26–0.85). Such a dramatic shift illustrates the influence of ocean biology on the chemical composition of particles in the size window most critical for aerosol–cloud interactions. Notably, this major shift occurred at modest TOC, chlorophyll-*a*, and phytoplankton levels (< 0.3 mg·m^{-3} and <7 × 10^3 cells·mL^{-1}). The transition was anticorrelated with chlorophyll-*a* and phytoplankton concentrations, and it was correlated with the onset of increasing bacteria concentrations (4 × 10^6 cells·mL^{-1}). In contrast, the chemical mixing state of SSA in larger sizes (180–320 nm) (Fig. 4*B*) showed less sensitivity to changes in bacteria, phytoplankton, and TOC concentrations. This result highlights the size-dependent response of SSA chemical composition and mixing state to changes in the distribution of and interactions between biological species in seawater. It also suggests that commonly used metrics for biological productivity in global atmospheric models and SSA parameterizations, such as ocean color and/or chlorophyll-*a* concentration, may not always represent adequate indicators of changes in SSA chemical composition and the associated climate-relevant properties that could be occurring under more typical ocean conditions (41, 42).

Impact of SSA Mixing State on Particle Hygroscopicity

Hygroscopicity measurements under both sub- and supersaturated conditions were performed during the mesocosm experiment. These measurement techniques probe water uptake of particles in different size ranges in the submicrometer mode. The ability of an individual particle to scatter radiation and/or serve as CCN depends on size, the degree of supersaturation, and the overall ability of a particle to uptake water, which depends on the single particle chemical mixing state. In general, particles composed mostly of water-soluble or hygroscopic salts will activate into cloud drops at relatively small sizes. As less soluble organic species are added to hygroscopic salt particles, the overall hygroscopicity decreases and the size at which the particles can activate increases. Particles that are composed of purely hydrophobic organic species will activate at even larger sizes (13). In previous marine cloud studies, the mixing state in the cloud-active size range (60–200 nm) has not been directly measured as a function of biological conditions. Bulk measurements of collections of SSA particles force one to assume all particles are internal mixtures of all seawater components in equal proportions, which suggests all SSA particles will have the same affinity for water. It is important to note that this will certainly not be the case for the different populations of nascent SSA particles described herein (12). The question we address here is as follows: How do biologically induced changes in the relative proportions of the two distinct submicrometer particle types (SS-OC and insoluble OC) affect hygroscopic properties?

Before adding bacteria and/or phytoplankton to the natural seawater, the measured mean activation diameter (d_{act}) at which particles began to serve as CCN was 63 nm (+18 nm, −4 nm; supersaturation of 0.2%), consistent with previous measurements for low biological activity seawater and the resulting hygroscopic SSA (12). Following a fivefold increase in bacteria concentrations that occurred ∼24 h after the initial addition of bacteria and ZoBell growth medium, the mean d_{act} nearly doubled to 118 ± 13 nm (Fig. 4*D*), corresponding to a factor of six decrease in the overall CCN-derived hygroscopicity (*SI Text*, section 5.2). Given the observed size distribution and relative fractions of inorganic and insoluble organic particles, this change in d_{act} values would result in a 32% decrease in the number of SSA particles that would activate as cloud droplets at 0.2% supersaturation. Because the size distribution showed very little change, the observed increase in d_{act} (Fig. 4*D*) directly

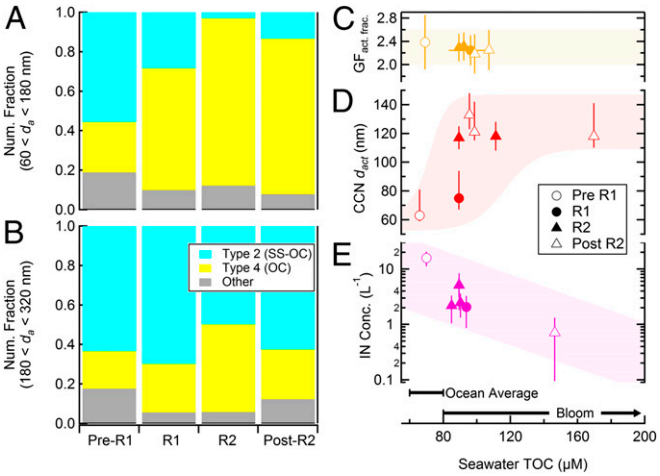

Fig. 4. (*A*) Single particle chemical mixing state for particles with a diameter between 60 and 180 nm for sampling regions indicated in Fig. 2 and Table S3 (the full dataset in these regions is discussed in *SI Text*, section 6). Num. fraction, number fraction. (*B*) Same as *A*, but for the next largest size regime (180 < d_p < 320 nm). (*C*) *GF* at 92% RH for the hygroscopic fraction of SSA ($GF_{act.\ frac.} = d_{wet}/d_{dry}$, act. frac. refers to the active fraction that took up water, *GF* >1.2), (*D*) d_{act} measured at 0.2% supersaturation for cloud droplet formation, and (*E*) IN concentrations (Conc.) at −32 °C as a function of seawater TOC levels. The shaded regions are provided as a visual guide. The data represent mean values, and the vertical error bars for *GF* and IN are 2σ. For CCN, the lower error bars are 2σ, whereas the upper bars account for potential errors in the counting mechanism used (*SI Text*, section 5.1). The horizontal error bars represent 1σ.

corresponds to a change in SSA chemical composition. More specifically, based on TEM analysis, the contributions from the two externally mixed particle types in the smallest <180-nm size range change with the relative fraction of type 4 insoluble OC particles increasing (Fig. 4*A*; 0.26–0.85) and replacing mixed SS-OC (type 2) particles. Notably, this observed decrease in hygroscopicity, which occurred under modest changes in bacteria, phytoplankton, TOC, and chlorophyll-*a* concentrations within the range of typical open ocean conditions, is significantly larger than in laboratory studies of nascent sea spray on the addition of biogenic material in the form of a variety of phytoplankton exudates (12). This large decrease in hygroscopicity occurred as the levels of two traditional indicators of high biological activity, phytoplankton and chlorophyll-*a*, were decreasing (6, 41). Little additional change occurred in CCN activity (Table S3) after phytoplankton were added when concentrations of chlorophyll-*a* (>5.5 mg·m^{-3}) exceeded the levels observed during most oceanic blooms (>2 mg·m^{-3}) (43). This result highlights the fact that bacteria and the full complexity of interactions between all biological species (e.g., phytoplankton, bacteria) must be included when probing seawater composition impacts on the concentration and composition of ocean-derived organic matter in SSA. The mesocosm experiment serves as an example of how this newly developed ocean-atmosphere wave flume approach will be used to determine cause-and-effect relationships between changing seawater composition and SSA mixing state.

To obtain complementary measurements of water uptake by larger submicrometer particles, subsaturated hygroscopic growth measurements of 175 to 225-nm dry diameter particles were made. Hygroscopic growth factor ($GF_{\text{act. frac.}} = d_{\text{wet}}/d_{\text{dry}}$) for the hygroscopic particle fraction ($GF > 1.2$) ranged from 2.2–2.4 at 92% RH, in the same range as SS (12). The *GF*s appeared to be independent of seawater composition (Fig. 4*C* and Fig. S6*A*). However, not all particles within this size range were hygroscopic, with 18 ± 4% displaying $GF < 1.2$, corresponding to 15-fold lower hygroscopicity compared with the highly hygroscopic particles (*SI Text* and Fig. S6*A*). The fraction of "nonhygroscopic" particles agrees well with the fraction of type 4 (OC) particles (0.25%) detected by TEM in the same size range (Fig. 4*B*), suggesting these are indeed hydrophobic (insoluble) organic particles as described by Facchini et al. (39). Additionally, despite the clear changes to the mean hygroscopicity of the smallest particles ($d_p < d_{act}$), no change occurred in the mean optically weighted *GF*s for all measured submicrometer particles measured using a cavity ring-down aerosol extinction spectrometer (Fig. S6*B*). This is consistent with the finding that the mean composition of the submicrometer SSA in the size range most relevant for light scattering and the direct aerosol effect on climate (300–1,000 nm) showed little dependence on changes in seawater composition (Fig. 4*B*). Our results suggest that under certain conditions, such as those simulated in these experiments, which are dominated by heterotrophic bacteria, a dichotomy of climate impacts can exist wherein certain changes in ocean composition due to biology can have a minimal influence on the optical properties of submicrometer SSA, although having a substantial impact on the indirect effect through modification of the hygroscopicity of particles with $d_p < d_{act}$, and hence cloud properties.

The final climate-relevant property probed as part of these studies of nascent SSA particles involves their ability to form IN. IN are rare; on average, only 1 in 10^5 particles serves as an ice nucleus below −22 °C (44). Some laboratory experiments and global aerosol modeling studies have investigated marine bacteria as potential sources of IN (45, 46), although our understanding of the actual chemical species influencing ice formation in SSA remains extremely limited. Observations of IN over marine regions show broadly distributed average IN concentrations of 10–20 per cubic meter active at −15 °C (47), increasing an order of magnitude per 5 °C drop in temperature, consistent with values measured in these experiments at −32 °C. Oceanic regions with higher IN concentrations have been suggested to be associated with higher biological activity, as indicated by chlorophyll-*a* or phytoplankton levels (46), but no definitive identification has been made of the specific sources of IN in marine environments. In this study, the dependence of IN concentrations on seawater conditions showed less variability than the CCN concentrations over the same range of conditions. The IN concentrations initially showed a small increase as bacteria concentrations increased but ultimately decreased at higher TOC levels above 100 μM (Fig. 4*E*). It is possible the high TOC levels created a sea surface film that inhibited the initial release of particles serving as IN. Our measurements showing the highest IN concentrations at the lowest TOC levels commonly observed in natural seawater suggest marine sources should be considered as a possible source of IN even outside of biologically active environments. However, further studies are needed to identify the sources leading to the modest yet globally significant marine IN source inferred from our studies and measured over a large fraction of the oceans.

Implications for Future Aerosol-Chemistry-Climate Studies

The development of this unique ocean-atmosphere facility sets the stage for future studies focused on improving our understanding of ocean–SSA–climate interactions. A number of key findings have emanated from the studies reported herein. First, the production rate and size distribution of SSA are extremely sensitive to the production mechanism, where bubbles with radii at and above the Hinze scale (a_H = 1.3 mm) are critical for SSA production, size, and composition. It is suggested that future studies aimed at producing SSA include measurements of bubble size distributions of the chosen production method to determine whether they fully emulate breaking waves, and that they include larger bubble sizes. Second, over a broad range of conditions, the mixing state of SSA is composed of varying fractions of four major externally mixed particle types, the number fractions of which are sensitive to ocean biology, and particularly the presence of heterotrophic bacteria, which have been shown to play a key role in consuming and transforming dissolved organic matter (48). Using this controlled approach, changes in the relative proportion of two externally mixed particle types (SS-OC and a second type dominated by insoluble organic species) occur, directly resulting in a change in the cloud formation potential of SSA. Interestingly, under the conditions of this experiment, the chemical composition and mixing state of particles larger than 180 nm did not demonstrate the same sensitivity to changes in seawater composition. This finding shows the importance of taking into account the size-resolved particle mixing state when predicting cloud properties in marine environments. Similar to the submicrometer hygroscopicity and optical property measurements, methods that measure bulk submicrometer mass of different chemical species will also be most strongly affected by the composition of larger, more massive particles at the upper end (>500 nm) of the submicrometer size mode (49), and thus relatively insensitive to changes in the number of particles in the size range most important for cloud formation (13).

The results of this study demonstrate the critical importance of using both the proper physical production mechanism that replicates breaking waves as well as a complete suite of biological species, including bacteria, phytoplankton, and viruses (48), to study factors controlling the concentration and composition of ocean-derived organic matter in SSA (40). Using the newly developed approach, studies will begin to study the coupling of ocean physical, biological, and chemical processes systematically, with the ultimate goal of linking seawater composition with SSA mixing state and cloud properties. This study represents a critical first step in producing and characterizing nascent SSA. Future studies will now focus on probing how rapidly these nascent SSA particles evolve by controlling a variety of atmospheric parameters, including photochemistry, aqueous phase processes, and heterogeneous chemistry with reactive trace gases. Finally, this ocean-atmosphere facility can be used to simulate how future changes in oceanic and atmospheric conditions may influence the chemical, physical, and climate-relevant properties of SSA.

Methods

To produce SSA particles with the identical size and composition of those in the atmosphere in a low-background environment, a unique ocean-atmosphere facility was developed that involved retrofitting a $33 \times 0.5 \times 1$-m wave channel housed at the Hydraulics Laboratory at the Scripps Institution of Oceanography. A significant effort was dedicated to reducing background particle concentrations (5,000–10,000 cm^{-3}) to low enough values (<20 cm^{-3}) so that individual SSA particles, produced in very low numbers (50–150 cm^{-3}) by each breaking wave, could be detected. SSA, generated from natural seawater, was sampled by multiple instruments within 30 s of being produced. Fig. S1 shows the wave channel with a multitude of gas and particle instruments probing SSA size, chemical mixing state, optical properties, hygroscopicity, and IN activity. Full details on the 5-d mesocosm experiment, including the source of the seawater, the methods used for seawater analyses, a discussion of the modifications to the existing wave channel that made it possible to detect low SSA concentrations, details of each of the particle generation methods, experimental procedures for measuring the bubble and aerosol size distributions, and analytical methods used for single particle measurements (including classification of particle types, supersaturated and subsaturated hygroscopicity measurements, and ice nucleation determinations) are provided in *SI Text*.

ACKNOWLEDGMENTS. We thank Suresh Dhaniyala, Robert Pomeroy, Paul Harvey, and the entire staff of the Scripps Institution of Oceanography Hydraulics Laboratory for helpful discussions and technical development of the sealed wave-channel. This overall study was supported by the National Science Foundation (NSF) Center for Chemical Innovation, the Center for Aerosol Impacts on Climate and the Environment (CAICE) under Grant CHE1038028. Partial support was provided to CAICE collaborators for the intensive study measurements by NSF Grant ATM0837913 (to C.D.C. and S.D.F.), Office of Naval Research Grant N00014-10-1-0200 (to J.H.S., S.P.H., and W.M.), an NSF Graduate Research Fellowship (to C.J.E.), an Irving M. Klotz professorship (to F.M.G.), NSF PO Grant OCE-1155123 (to G.B.D.), Gordon and Betty Moore Foundation Marine Microbiology Initiative (to F.A.) and NSF Grant ATM0841602 (to P.J.D. and R.C.S.).

1. Haywood J, Boucher O (2000) Estimates of the direct and indirect radiative forcing due to tropospheric aerosols: A review. *Rev Geophys* 38(4):513–543.
2. Intergovernmental Panel on Climate Change (2007). *Climate Change 2007: The Physical Science Basis*. Contribution of Working Group I to the Fourth Assessment Report of the Intergovernmental Panel on Climate Change, eds Solomon, S., D. Qin, M. Manning, Z. Chen, M. Marquis, K.B. Averyt, M. Tignor and H.L. Miller (Cambridge Univ Press, Cambridge, UK), pp. 129-234. Available at http://www.cambridge.org/features/earth_environmental/climatechange/wg1.htm.
3. Andreae MO (2007) Atmosphere. Aerosols before pollution. *Science* 315(5808):50–51.
4. Blanchard DC (1989) The ejection of drops from the sea and their enrichment with bacteria and other materials—A review. *Estuaries* 12(3):127–137.
5. Shank LM, et al. (2012) Organic matter and non-refractory aerosol over the remote Southeast Pacific: Oceanic and combustion sources. *Atmos Chem Phys* 12(1):557–576.
6. de Leeuw G, et al. (2011) Production flux of sea spray aerosol. *Rev Geophys* 49:RG2001.
7. Jaegle L, Quinn PK, Bates TS, Alexander B, Lin JT (2011) Global distribution of sea salt aerosols: New constraints from in situ and remote sensing observations. *Atmos Chem Phys* 11(7):3137–3157.
8. Lewis ER, Schwartz SE (2004) *Sea Salt Aerosol Production: Mechanisms, Methods, Measurements, and Models: A Critical Review* (American Geophysical Union, Washington, DC).
9. Leck C, Bigg EK (2005) Biogenic particles in the surface microlayer and overlaying atmosphere in the central Arctic Ocean during summer. *Tellus B Chem Phys Meterol* 57(4):305–316.
10. Parungo FP, Nagamoto CT, Rosinski J, Haagenson PL (1986) A study of marine aerosols over the Pacific-ocean. *J Atmos Chem* 4(2):199–226.
11. O'Dowd CD, et al. (2004) Biogenically driven organic contribution to marine aerosol. *Nature* 431(7009):676–680.
12. Fuentes E, Coe H, Green D, McFiggans G (2011) On the impacts of phytoplankton-derived organic matter on the properties of the primary marine aerosol. Part 2. Composition, hygroscopicity and cloud condensation activity. *Atmos Chem Phys* 11(6):2585–2602.
13. Andreae MO, Rosenfeld D (2008) Aerosol-cloud-precipitation interactions. Part 1. The nature and sources of cloud-active aerosols. *Earth Sci Rev* 89(1-2):13–41.
14. Hawkins LN, Russell LM (2010) Polysaccharides, proteins, and phytoplankton fragments: Four chemically distinct types of marine primary organic aerosol classified by single particle spectromicroscopy. *Adv Meteorol* 2010:1–14.
15. Murphy DM, et al. (1998) Influence of sea-salt on aerosol radiative properties in the Southern Ocean marine boundary layer. *Nature* 392(6671):62–65.
16. Bigg EK, Leck C (2008) The composition of fragments of bubbles bursting at the ocean surface. *J Geophys Res Atmos* 113(D11):D11209.
17. Ellison GB, Tuck AF, Vaida V (1999) Atmospheric processing of organic aerosols. *J Geophys Res Atmos* 104(D9):11633–11641.
18. Griffith EC, Tuck AF, Vaida V (2012) Ocean-atmosphere interactions in the emergence of complexity in simple chemical systems. *Acc Chem Res* 45(12):2106–2113.
19. Deane GB, Stokes MD (2002) Scale dependence of bubble creation mechanisms in breaking waves. *Nature* 418(6900):839–844.
20. Hansell DA, Carlson CA, Repeta DJ, Schlitzer R (2009) Dissolved organic matter in the ocean a controversy stimulates new insights. *Oceanography (Wash DC)* 22(4):202–211.
21. Li WKW (1998) Annual average abundance of heterotrophic bacteria and Synechococcus in surface ocean waters. *Limnol Oceanogr* 43(7):1746–1753.
22. Boyce DG, Lewis MR, Worm B (2010) Global phytoplankton decline over the past century. *Nature* 466(7306):591–596.
23. Aller JY, Kuznetsova MR, Jahns CJ, Kemp PF (2005) The sea surface microlayer as a source of viral and bacterial enrichment in marine aerosols. *J Aerosol Sci* 36(5-6):801–812.
24. Schmitt-Kopplin P, et al. (2012) Dissolved organic matter in sea spray: A transfer study from marine surface water to aerosols. *Biogeosciences* 9(4):1571–1582.
25. Keene WC, et al. (2007) Chemical and physical characteristics of nascent aerosols produced by bursting bubbles at a model air-sea interface. *J Geophys Res-Atmos* 112: D21202.
26. Sellegri K, O'Dowd CD, Yoon YJ, Jennings SG, de Leeuw G (2006) Surfactants and submicron sea spray generation. *J Geophys Res Atmos* 111(D22):D22215.
27. Cipriano RJ, Blanchard DC (1981) *Bubble and aerosol spectra produced by a laboratory breaking wave. J Geophys Res C Oceans Atmos* 86(Nc9):8085–8092.
28. Resch FJ, Darrozes JS, Afeti GM (1986) Marine liquid aerosol production from bursting of air bubbles. *J Geophys Res Oceans* 91(C1):1019–1029.
29. Wu J (2001) Production functions of film drops by bursting bubbles. *J Phys Oceanogr* 31(11):3249–3257.
30. Fuentes E, Coe H, Green D, de Leeuw G, McFiggans G (2010) Laboratory-generated primary marine aerosol via bubble-bursting and atomization. *Atmospheric Measurement Techniques* 3(1):141–162.
31. Yoon YJ, et al. (2007) Seasonal characteristics of the physicochemical properties of North Atlantic marine atmospheric aerosols. *J Geophys Res Atmos* 112(D4):D04206.
32. Clarke AD, Owens SR, Zhou JC (2006) An ultrafine sea-salt flux from breaking waves: Implications for cloud condensation nuclei in the remote marine atmosphere. *J Geophys Res Atmos* 111(D6):D06202.
33. Bates TS, et al. (2012) Measurements of ocean derived aerosol off the coast of California. *J Geophys Res Atmos* 117:D00V15.
34. Gantt B, Meskhidze N, Zhang Y, Xu J (2010) The effect of marine isoprene emissions on secondary organic aerosol and ozone formation in the coastal United States. *Atmos Environ* 44(1):115–121.
35. Murphy DM, Thomson DS, Middlebrook AM, Schein ME (1998) In situ single-particle characterization at Cape Grim. *J Geophys Res Atmos* 103(D13):16485–16491.
36. Tang CY, Huang ZSA, Allen HC (2010) Binding of $Mg^{(2+)}$ and $Ca^{(2+)}$ to palmitic acid and deprotonation of the COOH headgroup studied by vibrational sum frequency generation spectroscopy. *J Phys Chem B* 114(51):17068–17076.
37. Gaston CJ, et al. (2011) Unique ocean-derived particles serve as a proxy for changes in ocean chemistry. *J Geophys Res Atmos* 116:D18310.
38. Matthias-Maser S, Brinkmann J, Schneider W (1999) The size distribution of marine atmospheric aerosol with regard to primary biological aerosol particles over the South Atlantic Ocean. *Atmos Environ* 33(21):3569–3575.
39. Facchini MC, et al. (2008) Primary submicron marine aerosol dominated by insoluble organic colloids and aggregates. *Geophys Res Lett* 35(17):L17814.
40. Verdugo P (2012) Marine microgels. *Annu Rev Mar Sci* 4:375–400.
41. Gantt B, et al. (2012) Model evaluation of marine primary organic aerosol emission schemes. *Atmos Chem Phys* 12(18):8553–8566.
42. O'Dowd CD, et al. (2008) A combined organic-inorganic sea-spray source function. *Geophys Res Lett* 35(1):L01801.
43. Chavez FP, Messié M, Pennington JT (2011) Marine primary production in relation to climate variability and change. *Annu Rev Mar Sci* 3:227–260.
44. DeMott PJ, et al. (2010) Predicting global atmospheric ice nuclei distributions and their impacts on climate. *Proc Natl Acad Sci USA* 107(25):11217–11222.
45. Burrows SM, Hoose C, Pöschl U, Lawrence MG (2012) Ice nuclei in marine air: biogenic particles or dust? *Atmos Chem Phys Discuss* 12(2):4373–4416.
46. Schnell RC, Vali G (1976) Biogenic ice nuclei. 1. Terrestrial and marine sources. *J Atmos Sci* 33(8):1554–1564.
47. Bigg EK (1973) Ice nucleus concentrations in remote areas. *J Atmos Sci* 30(6): 1153–1157.
48. Azam F (1998) Microbial control of oceanic carbon flux: The plot thickens. *Science* 280(5364):694–696.
49. Ovadnevaite J, et al. (2012) On the effect of wind speed on submicron sea salt mass concentrations and source fluxes. *J Geophys Res Atmos* 117:D16201.